

Reinforcement learning-based architecture search for quantum machine learning

Frederic Rapp^{1,2}, David A. Kreplin¹, Marco Roth^{1*}

¹Fraunhofer Institute for Manufacturing Engineering and Automation (IPA), Nobelstrasse 12, Stuttgart, 70569, Germany.

²Institute of Industrial Manufacturing and Management IFF, University of Stuttgart, Allmandring 35, Stuttgart, 70569, Germany.

*Corresponding author(s). E-mail(s): marco.roth@ipa.fraunhofer.de;
Contributing authors: frederic.rapp@ipa.fraunhofer.de;

Abstract

Quantum machine learning (QML) leverages the large Hilbert space provided by quantum computing for data encoding, typically realized by parameterized quantum circuits (PQCs). While classical machine learning deals extensively with problem-specific model design, QML models mainly use hardware-efficient and heuristic circuit designs for PQCs. This work presents a novel approach employing the reinforcement learning algorithm MuZero to generate problem-specific PQCs to improve the QML performance. Diverging from previous search algorithms, we adopt a layered circuit design to significantly reduce the search space. Furthermore, we utilize cross-validation scoring to train the reinforcement learning algorithm, rewarding the discovery of high-performing circuits. In benchmarks we compare our tailored circuits with reference circuits from the literature, randomly generated circuits, and circuits generated by genetic algorithms. Our findings underscore the efficacy of problem-tailored encoding circuits in enhancing QML model performance.

Keywords: quantum computing, quantum machine learning, reinforcement learning, architecture search

1 Introduction

Quantum machine learning (QML) is a promising application of today's noisy intermediate-scale quantum (NISQ) computing [1], and has gained significant attention in recent years [2]. Most QML methods rely on encoding data into the high-dimensional Hilbert space accessible through quantum computing [3, 4]. Parameterized quantum circuits (PQCs) [5], which use parameterized gates that depend on input data and trainable weights, have become a focus of recent research to encode data. The weights are often optimized through an

optimization loop based on traditional routines [6]. However, the high dimensionality of Hilbert spaces can lead to exponentially vanishing gradients if the quantum circuit is not chosen properly [7, 8]. PQCs, in the following also denoted as encoding circuits, are central to many methods used in QML, such as quantum neural networks (QNNs) [5, 9] and quantum kernel methods [3, 10, 11]. Various encoding strategies, such as data re-uploading or non-linear encoding, have been introduced in the literature [12–15]. In contrast to other applications of PQCs in variational algorithms, such as optimization with the quantum approximate

optimization algorithm (QAOA) [16] or quantum simulations using the variational quantum eigensolver (VQE) [17, 18], the circuits used in QML offer a high degree of flexibility, allowing for adaptation to specific hardware configurations, such as connectivity or native gates. Commonly used architectures often share properties like a layered structure where each qubit is acted upon by the same operation simultaneously [19]. Current designs are often based on these design principles only, and are not necessarily tailored for optimal model performance.

This heuristic design of QML models contrasts with the no free lunch theorem [20], which asserts that optimal performance is achieved by a problem specific model. Studies have shown that generic QML models often fail to outperform classical ML approaches [21, 22]. As a result, recent research has focused on incorporating geometric properties, such as symmetries, into QML architectures to provide models with a informed inductive bias [23–26]. Nonetheless, many of these approaches require expert knowledge of problem domains and quantum circuit design, a prerequisite shared by other informed design choices [27]. Despite existing works discussing the necessity of considering structure data structure in PQCs [22], there are no established guidelines for constructing suitable PQCs for specific QML problems. This gap motivates the development of automated methods that can create and evaluate different encoding circuits, capable of generating problem-specific encoding circuits from input data. Current research primarily employs genetic algorithms for this architecture search [28–30].

In this work, we introduce a novel approach for QML circuit generation using model-based reinforcement learning (RL) with the MuZero algorithm [31]. In RL, an agent develops a policy by interacting with an environment to maximize cumulative rewards. For circuit generation, the observation space includes the current circuit, actions determine the next layer of quantum gates, and rewards are based on the QML model’s training performance measured by the cross-validation score. MuZero uses deep neural networks to map the interaction between circuit architecture and QML model performance into a hidden state representation, significantly reducing the need for detailed environmental information. Actions are

selected in a Monte Carlo Tree Search (MCTS) [32] fashion, which relies on internal actions and rewards, reducing the number of evaluations of the QML model. Figure 1 illustrates our method’s conceptual layout. We demonstrate through benchmarks that the MuZero circuit search algorithm can generate problem-specific encoding circuits that surpass both reference circuits from the literature and those derived from random sampling or genetic search algorithms [28]. The results are consistently favorable across three different datasets: two involving regression tasks and one classification task. The resulting QML models, which utilize projected quantum kernels (PQKs) [11], exhibit performance that is either comparable to or slightly superior to various classical ML models.

The remainder of this work is structured as follows. In Section 1.1, we provide an overview of prior work in the field of quantum architecture search. Section 2 defines the general problem setting and elaborates the MuZero circuit search algorithm. In Section 3, we demonstrate the versatility and circuit-creating capabilities of our algorithm by benchmarking it on several datasets. Finally, we discuss the results of the MuZero circuit search algorithm in Section 3.2.

1.1 Prior work

The integration of RL techniques into quantum circuit design has been explored in various approaches. One key aspect focuses on optimizing quantum circuits to meet quantum hardware requirements, such as reducing gate count or enhancing qubit routing efficiency [33]. A notable contribution in the area of general quantum circuit optimization is the methodology proposed by Ruiz et al. [34], which employs tensor networks to reduce the number of gates in quantum circuits. This framework focuses on minimizing the gate overhead in deep circuit architectures, thereby facilitating practical implementations on quantum hardware.

The integration of RL techniques into quantum circuit design has been explored by [35] and [36]. The first study [35] applies RL techniques to create and optimize quantum circuits for VQE, aiming to enhance accuracy while maintaining a low circuit depth. Ref. [36] addresses the challenges associated with using RL for quantum circuit design, introducing the concept of using Markov decision processes to guide the application of continuously

parameterized quantum gates to optimize quantum circuits, specifically in the context of quantum state preparation. While these studies utilize RL for quantum circuit architecture search, their primary applications lie outside of QML. Additionally, in contrast to our work, they rely on model-free RL approaches.

In the context of QML, quantum circuit design has been investigated in the following two references. Incudini et al. [29] propose an architecture search for quantum kernels, wherein they employ techniques from neural architecture search and AutoML. They demonstrate the effectiveness of automated methods over manual design approaches, as illustrated by their experiments with high-energy physics datasets. Among other techniques, such as Bayesian optimization, they also employ RL optimization based on a model-free state-action-reward-state-action (SARSA) algorithm. Ref. [28] introduces a multiobjective genetic algorithm for the automatic generation of quantum feature maps for fidelity-based quantum kernels. We include a slightly modified version of their implementation in our benchmarks in Sec. 3.1.

Notably, our research incorporates and extends upon these methodologies. In contrast to previous works, we focus on a layered approach that considerably reduces the search space. Furthermore, we employ model-based RL to decrease the number of circuit evaluations by incorporating the MuZero algorithm [31].

2 Methods

This study focuses on supervised learning where a model is trained on a data set $\mathcal{D} = (X, y)$, with $X = \{\mathbf{x}_1, \dots, \mathbf{x}_N\}$ comprising N data points $\mathbf{x}_i \in \mathcal{X} \subset \mathcal{R}^d$ with corresponding labels $y_i \in \mathcal{Y}$. We address regression problems with $\mathcal{Y} \subset \mathbb{R}$, and binary classification tasks with $\mathcal{Y} = \{0, 1\}$. Quantum machine learning models such as QNNs or quantum kernel methods rely on embedding data $\mathbf{x} \in \mathcal{X}$ into quantum states

$$\rho(\mathbf{x}, \boldsymbol{\theta}) = U(\mathbf{x}, \boldsymbol{\theta})\rho_0U(\mathbf{x}, \boldsymbol{\theta})^\dagger, \quad (1)$$

with $\rho_0 = |0\rangle\langle 0|$. From this definition one can derive QML models with respect to some observable O as

$$f(\mathbf{x}, \boldsymbol{\theta}) = \text{tr}(\rho(\mathbf{x}, \boldsymbol{\theta})O). \quad (2)$$

The operator $U(\mathbf{x}, \boldsymbol{\theta})$ is typically realized by a quantum circuit, and can be expressed as a product of unitary operators

$$U(\mathbf{x}, \boldsymbol{\theta}) = \prod_{l=1} V_l(\mathbf{x}, \boldsymbol{\theta}), \quad (3)$$

where $V_l(\mathbf{x}, \boldsymbol{\theta}) = \exp(-i\phi(\mathbf{x}, \boldsymbol{\theta})H_l)$. Here H_l is a traceless Hermitian operator and ϕ is a (potentially) non-linear function of the parameters and the data. Note that this include the simple cases $\phi = x^j$ and $\phi = \theta^j$, where x^j (θ^j) is the j -th component of a datapoint \mathbf{x} (parameter vector $\boldsymbol{\theta}$).

A model of the form of Eq. (2) can be trained directly by minimizing an appropriate loss function or used as a variant of quantum pre-processing, as for example in projected quantum kernels [11, 37]. From Eqs. (2)–(3) it becomes clear that the choice of PQCs plays a defining role in the model's general architecture. To account for the current hardware restrictions in the NISQ regime, the set of operators \mathcal{V} from which the operators V_l in Eq. (3) are chosen is often restricted to the native gate set of a specific hardware, resulting in hardware-efficient circuits which require a minimal amount of transpilation.

The choice of circuit architecture profoundly impacts the properties of the resulting model. For example, the expressivity of QML models is tightly connected to the circuit structure [38]. Also, certain encoding circuits in quantum kernel methods can cause the quantum kernel to resemble a classical kernel, losing potential quantum advantage [39]. Therefore, the choice of operators and their placement in the encoding circuit is crucially important to the overall performance of the QML model. Despite its importance, this aspect is often neglected. A notable exception where informed architecture design is used is geometric QML. Here symmetries in the data are reflected in the design of the circuit, resulting in models with desirable properties such as good generalization and trainability [23–26, 40]. However, tailoring the encoding requires deep knowledge about the underlying properties of the dataset, which is often intractable. For general data sets and ML problems, the choice of circuit architecture is therefore an open question which is usually not addressed beyond heuristics. It is desirable to create encoding circuits that are not solely reliant on hardware efficiency but also consider the model's performance on the specific problem.

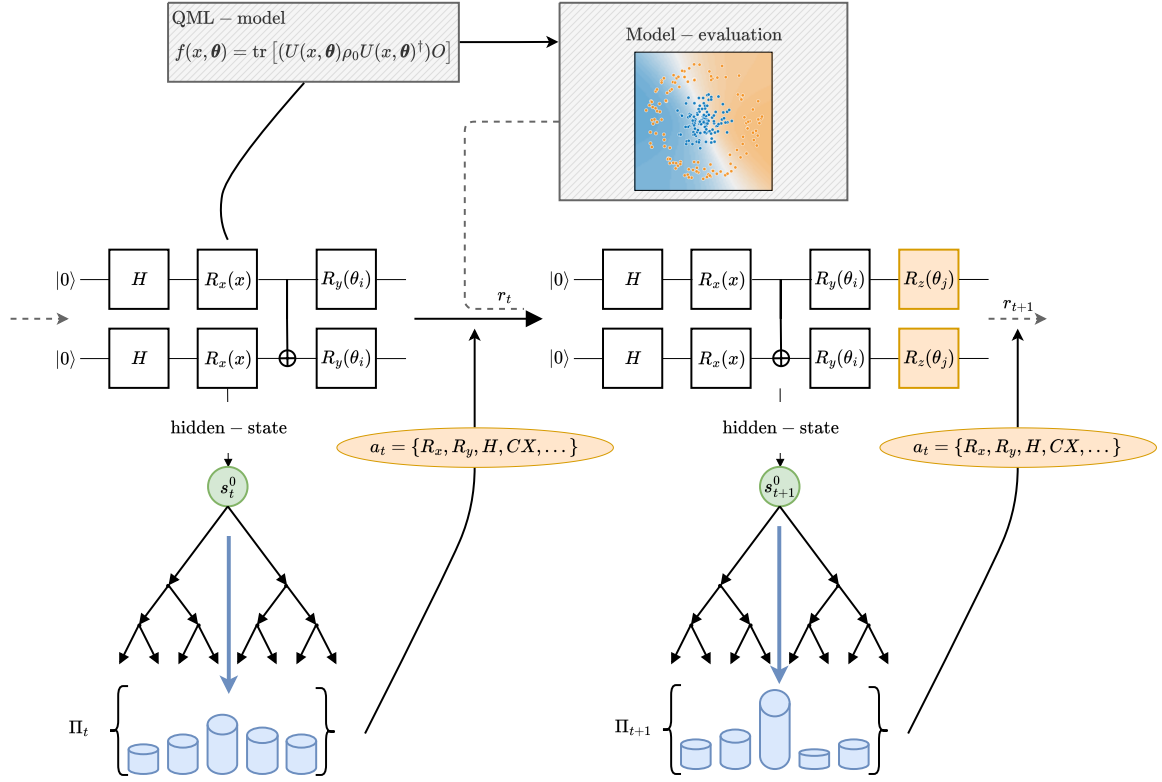


Fig. 1 Automatic PQC generation layout. The MuZero model observes the current PQC configuration, and transforms it into a hidden state representation s_t^n . By performing an MCTS for each time step t the model obtains a policy Π_t from which a action a_t is sampled [31]. The action represent a choice of unitary operator (e.g., H, CX, \dots) which is appended on the current encoding circuit in a layered fashion (one gate for each qubit). Each circuit observation is used as basis for a QML model of the form presented in Eq. (2). Based on the cross-validation score the MuZero agent receives a reward r_t at each time step.

In this work, we employ the RL algorithm MuZero to build encoding circuits. The algorithm creates encoding circuits iteratively by choosing and placing unitary operators such that the performance of a resulting QML model is optimized. The individual components of the framework will be discussed in the following, an overview of the algorithm can be found in Fig. 1.

2.1 Model-based reinforcement learning algorithm

Generally, a RL agent interacts with its environment by taking actions a_t at each time step t and receiving a reward r_t in return. The agent's objective is to optimize its policy $\Pi_t(a_{t+1}|o_1, \dots, o_t, a_1, \dots, a_t)$, which describes the

probability of taking an action a_{t+1} given previous observations o_1, \dots, o_t and actions a_1, \dots, a_t , in order to maximize cumulative rewards. RL encompasses a variety of approaches [41] which can be categorized into model-free approaches like proximal policy optimization [42] and model-based techniques such as model predictive control [43] or the MuZero algorithm [31].

The general workflow of the MuZero algorithm transforms the observation, in our case the current encoding circuit, into a hidden state representation, which comprises a dynamics function, a prediction function, and a representation function—all based on deep neural networks. At each time step t , the model processes this hidden state for $k = 1, \dots, K$ steps and computes an internal reward, a value function, and a policy based on the network's

predictions in an MCTS fashion. At the end of each MCTS step, an action is sampled from the policy $p_t^k = \Pi_t(a_{t+k+1}|o_1, \dots, o_t, a_t + 1, \dots, a_t + k)$, and the actual reward and value function are computed. The weights of the three networks are optimized during the training process to minimize the difference between the internal hidden state predictions and real outcomes. For more detail on the algorithm, we refer to [31].

The transformation of the observation space into a hidden state does not impose strong restrictions on capturing the dynamics of the environment, essentially interpreting the abstract process as a hidden layer of a deep neural network. This characteristic makes the algorithm suitable for QML, where full information about the complex dynamics of the interaction between PQCs and data problems is not fully known. Another critical aspect is its scalability in computational resources. The algorithm approximates all necessary functions using classical neural networks, thereby minimizing calls to the QML environment, typically the primary computational bottleneck in the NISQ era. In the next section, we provide a detailed explanation on how MuZero can be utilized to generate encoding circuits that achieve good performance.

2.2 Encoding circuit generation

The overall workflow of the circuit generation process based on MuZero, denoted in the following as MuZero circuit search, is shown in Fig. 1. The RL agent builds quantum circuits in a layered structure, where each gate operator is applied to every accessible qubit in a layered fashion. Two-qubit gates are considered in a linear nearest neighbour entangling configuration between the qubits. An exemplary layout of the layered structure is shown in Fig. 2. Although a more flexible structure is generally possible, it comes with the caveat of a rapidly growing search space, in which good solutions might be rare to find. In addition, we have found the layered structure to perform very well in our benchmark calculations compared to a flexible structure as is discussed in more detail in Section 3.2.

The action set of the RL framework, i.e., the set of gates available to the agent, is listed in Table 1. While additional one and multi-qubit gates could be considered, we limit the selection to those primarily used in PQCs for QML to reduce the search

space. Rotational gates are employed to encode input features or manipulate the quantum state. Besides linear data encoding, we also included gates with nonlinear transformations of the data using $\tan^{-1}(x)$. In our approach, we avoid trainable weights and instead use fixed angles. This allows the MuZero circuit search to optimize the angles implicitly by selecting gates and angles that lead to an optimal reward. The fixed angles are given by $\frac{\pi}{n}$ with $n \in \{1, 2, 3, 4, 8\}$. The total number of qubits must be predefined and, in our implementation, is always the number of features of the ML problem, ensuring that each feature is represented once in every layer. While it is conceptually reasonable to allow the agent to choose the number of qubits, we do not consider this to reduce the complexity of the actions.

The environment of the RL agent is initialized by an empty circuit with all qubits initialized in the zero state. The agent then iteratively adds gates until a specified number n_{maxdepth} of layers has been reached which triggers a resets of the environment. Furthermore, we found it beneficial to incorporate random initial architectures to improve the agent's exploration capabilities. These random restarts are executed with a probability of 20%, and they are achieved by randomly picking $n_{\text{maxdepth}}/2$ actions and ensuring that at least one feature encoding layer is included.

The reward for the RL agent is determined based on the cross-validation score of the QML model utilizing the generated circuit. This approach aims to avoid creating circuits that could lead to overfitting. The specific metric for the cross-validation value may vary depending on the type of problem. The agent is granted the highest reward for surpassing the overall highest found score. Similarly, a substantial reward is provided for reproducing the best-known result. A lower reward is given for improving the result within the limits of the current environment, with the reference value being reset in each new environment. A minor penalty is applied if the score does not improve, encouraging the development of shorter circuits. A major penalty is imposed if the encoding circuit does not contain any gates dependent on \mathbf{x} . In such cases, the cross-validation evaluation is also skipped.

In principle, the presented MuZero circuit search algorithm is independent of the QML model. For practical reasons, in the reaming work we

X	CX	$R_x(\pi x)$	$R_x(\frac{\pi}{n})$
Y	CY	$R_y(\pi x)$	$R_y(\frac{\pi}{n})$
Z	CZ	$R_z(\pi x)$	$R_z(\frac{\pi}{n})$
H	$CR_x(\frac{n\pi}{8})$	$CR_y(\frac{\pi}{n})$	$CR_z(\frac{\pi}{n})$
$R_x(\tan^{-1}(x))$	$R_y(\tan^{-1}(x))$	$R_z(\tan^{-1}(x))$	

Table 1 Set of gates which can be chosen as actions by the RL agent. Gates are added as layers to all qubits at the end of the circuit, two-qubit gates are considered in a linear nearest neighbor entangling configuration.

Parameterized gates are available for $n \in \{1, 2, 3, 4, 8\}$

focus exclusively on QML models based on projected quantum kernels (PQKs), as they provide a robust QML framework that is quick to evaluate. PQKs use quantum states as an intermediate step and project back to classical representations using observables before evaluating the kernel. This process can be viewed as preprocessing the input data by the quantum model before applying a classical kernel method. We employ a Gaussian outer kernel with 1-reduced-density matrices as proposed in Ref. [11]:

$$K^{\text{PQK}}(\mathbf{x}, \mathbf{x}') = \exp \left(-\gamma \sum_{O,k} [f_{O,k}(\mathbf{x}) - f_{O,k}(\mathbf{x}')]^2 \right). \quad (4)$$

Here, $\gamma > 0$ is a hyperparameter of the kernel, and $f_{O,k} = \text{tr}(\rho(\mathbf{x})O_k)$, where the observable O_k is taken from the set of single-qubit Pauli matrices $\{X, Y, Z\}$ and applied to qubit k . We primarily chose PQKs for two reasons: they are efficient to evaluate and have shown good results for various ML tasks. Unlike fidelity quantum kernels that are based on the overlap of the two quantum states [10], the evaluation of quantum circuits with PQKs scales linearly with the data. Additionally, caching of intermediate results enables a fast evaluation of the cross-validation score. In contrast to PQKs, QNNs require an expensive training routine that involves numerous evaluations of quantum circuits for each training data point, making the search for optimal architectures prohibitive. The implementation of the circuits, the PQK, and the QML models is achieved using the QML library *sQULearn* [44].

3 Results

To benchmark the capabilities of the MuZero circuit search, we compare the performance of the generated circuits to reference encoding circuits

used in the literature [12–15]. Additionally, we compare the results to those obtained by generating encoding circuits with a genetic algorithm [28], as well as circuits with randomly chosen gate sequences. Furthermore, we compare these results to those from various classical machine learning models. Our approach is evaluated across three distinct datasets, including two regression tasks and one classification task.

3.1 Benchmark set-up

This section details the setup of our benchmark calculations, which is consistent across all compared methods and circuits. First, the dataset is split into two parts: a training set and a test set. The training set is used to determine suitable encoding circuits and optimize the hyperparameters of the underlying (Q)ML model. The test data is reserved solely for calculating the final score, which is used for comparing the different approaches. The architecture search algorithms, including the MuZero circuit search algorithm, random searches, and the genetic algorithm, follow a three-step approach:

1. Generation and selection: We generate various circuits and select the five best circuits based on the cross-validation score on the training data.
2. Hyperparameter optimization: We optimize the hyperparameters of the underlying (Q)ML model using the cross-validation score of the training data.
3. Final evaluation: We train the final model on the full training data and evaluate the final score using the test data.

The cross-validation in steps (1) and (2) utilizes the R^2 score for regression tasks and accuracy for the classification example, based on five fixed folds for every dataset. The hyperparameters in step (1) are consistent across all architecture search algorithms. The hyperparameter optimization in step (2) is performed using the Optuna library [45], optimizing both the hyperparameters of the (Q)ML model and the hyperparameter γ of the PQK. The number of executed cross-validations is comparable for all architecture search algorithms and is in the order of 10^5 evaluations. For reference circuits from the literature, step (1) is replaced by optimizing the variational parameters of the PQCs with target alignment (cf. Sec. 3.1.4). For classical ML models, step (1) is not required. All results in this work

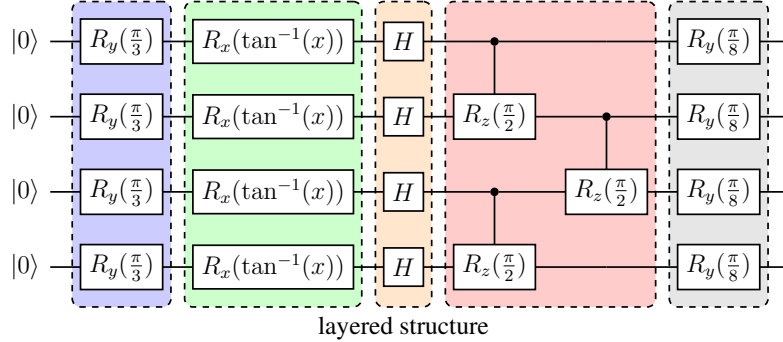


Fig. 2 Example of the layered circuit structure with $q = 4$ qubits that has been created after 5 actions of the RL agent. The operators are chosen out of the action set described in Tab. 1. Different configurations of layered approach are used for the results in this paper.

are obtained using ideal statevector simulations. In the following, we discuss details specific to each method.

3.1.1 MuZero circuit search

The MuZero circuit search algorithm employs a maximum of $n_{\text{maxdepth}} = 10$ layers to maintain hardware efficiency. The final encoding circuits are obtained from those generated during both the training and inference phases of the MuZero search algorithm, in which the algorithm’s weights remain fixed during inference.

3.1.2 Random encoding circuits

Random circuits are generated using two distinct methodologies: the layered approach of the MuZero circuit search and a fully flexible structure. We utilize the same gate set as employed in the RL algorithm (cf. Tab. 1) and construct random layered structures as illustrated in Fig. 2 and detailed in Section 2.2, by randomly selecting between 2 and $n_{\text{maxdepth}} = 10$ actions. Moreover, we generate circuits based on a flexible structure that do not adhere to a layer-wise application of gates. In this fully random approach, one- and two-qubit gates are placed at every possible position within the circuit. The rotation angles of individual gates are randomly sampled from a uniform distribution between $[0, 2\pi]$. The maximum number of placed gates mirrors the total number of gates in the layered approach. Additionally, we ensure that all features in \mathbf{x} are encoded at least once in the circuits, a prerequisite for the MuZero circuit search algorithm to learn. For both random generation

methods, we sample 10,000 circuits and select the top 5 circuits based on the cross-validation score of the training data.

3.1.3 Genetic algorithms

We compare our approach with the genetic algorithm proposed in [28], incorporating a slight modification in the selection of the quantum kernel. While [28] employs fidelity-based quantum kernels, we integrate PQKs into the algorithm. Furthermore, we adjust the training procedure to prioritize the cross-validation score, departing from the original methodology that relies on training and testing scores, in order to align with the RL and random search methods. The genetic algorithm is not bound to the layered circuit structure. It has a high level of flexibility when building circuits, e.g. it can encode multiple features on one qubit wire, as well as having full freedom in placing entangling gates, as described in detail in Ref. [28].

3.1.4 Reference circuits

Additionally, we benchmark our findings against popular circuits found in the literature [12–15]. We use four different circuits including a data-reuploading scheme which has been successful in previous QML studies [12, 46]. With the exception of one circuit, all others circuits feature variational parameters θ that we optimize by maximizing the kernel-target-alignment (TA) metric [12, 47] over

the training set:

$$\text{TA}(K) = \frac{\sum_{i,j} K(\mathbf{x}_i, \mathbf{x}_j) y_i y_j}{\sqrt{\sum_{i,j} K(\mathbf{x}_i, \mathbf{x}_j)^2 \sum_{i,j} y_i^2 y_j^2}},$$

where K represents the data-dependent Kernel matrix (cf. Eq. (4)). The chosen reference circuits provide a overview of prevalent strategies found in the literature, encompassing design principles such as hardware-efficient entanglement and the placement of trainable variational parameters within the circuits.

3.1.5 Classical models

We employ various classical ML models, including SVMs, Artificial Neural Networks, Random Forests, Gradient Boosting, and Kernel Ridge Regression for regression tasks. Specifically, Gradient Boosting is implemented utilizing the XGBoost library [48], while neural networks are constructed using the TensorFlow library [49]. The remaining models leverage the scikit-learn library [50]. Hyperparameter optimization for all classical models is conducted via the Optuna library [45] on the training dataset, employing cross-validation techniques.

3.1.6 Data sets

We evaluate all models on three data sets, two regression problems and one classification problem. The number of qubits in the QML algorithms is equal to the number of features.

The *California housing* data set from scikit-learn [50] is a regression problem that aims to predict the prices of houses in California. The data is scaled in a range of $[0, 1]$, and we choose a fixed sub set of $n_{\text{data}} = 1,000$ randomly chosen data points. These data points are partitioned into $n_{\text{training}} = 700$ training points and $n_{\text{test}} = 300$ test points. The dataset has 8 features.

The *Quantum fashion MNIST* (QFMNIST) data set is based on the fashion-MNIST data set [51], and prepared in a quantum state as described in [11]. This essentially creates a regression problem for an artificial quantum data set. The data is re-scaled to zero mean and unit variance, and the original features are reduced using scikit-learn's PCA implementation [50] using the first 4 principal components as features. We use

$n_{\text{training}} = 100$ training points, and $n_{\text{test}} = 100$ test points, that are scaled in a range from $[-1, 1]$.

The *Two-curves (diff)* data set [46] is a classification task which models the curvature and the minimum distance of two curves in a d -dimensional space. Here, we follow the data creation procedure given in [46]. The problems' difficulty can vary depending on the choice of degree and the number of features. We use the most difficult version of the data set described in [46] using 10 features and a degree of 20. The data is re-scaled to zero mean and unit variance. We use $n_{\text{data}} = 300$ samples and split them into $n_{\text{training}} = 240$ training points for cross-validation, and $n_{\text{test}} = 60$ test points.

3.2 Experiments

Fig. 3 displays the R^2 scores of the two regression datasets. For the California housing data (Fig. 3(a)), the best overall performance is achieved by the QSVR approach utilizing the encoding circuits generated by the MuZero circuit search algorithm. This approach outperforms the encoding circuits generated by random search and the genetic algorithm. The best QML models utilizing the reference circuits perform about as well as the best classical model for this task. Classical ML models, shown in the first column and labeled as CML in Fig. 3(a), have the largest performance range. The best CML model is the SVR, with an $R^2_{\text{SVR}} = 0.752$ test score.

We observe a similar behavior for the QFMNIST regression problem. As can be seen in Fig. 3(b), the best performance is obtained with the circuits found with the MuZero circuit search algorithm, followed by circuits constructed with the genetic algorithm. The use of reference circuits yield good solutions, however, some of the chosen reference circuits lead to significantly underperforming models. In contrast to Fig. 3(a), in which the best reference has no trainable parameters [13], the same circuit in Fig. 3(b) shows the worst results among all encoding circuits considered. For the QFMNIST data, QML models perform better than the best classical ML model. This is because this data set is a synthetic data set specifically designed to be difficult to simulate classically. [11]

The third benchmark is a classification task on the *two-curves (diff)* dataset from [46], with the settings described in Sec. 3.1.6. Figure 4 showcases the models' performance measured by the accuracy

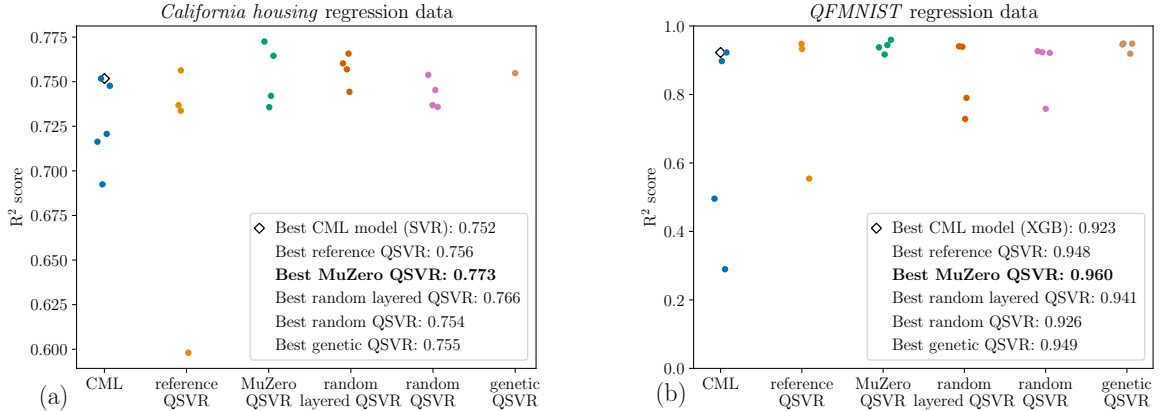


Fig. 3 Performance of the regression (Q)ML models; (a) *California housing* test data, and (b) *QFMNIST* test data. The first category marks the results of different classical ML models, as described in Sec. 3.1.5. The second category shows the results of a QSVR based on a variety of reference encoding circuits (Sec. 3.1.4). The third shows the results of the QSVR based on encoding circuits built by the MuZero circuit search (Sec. 2.2). The fourth and fifth columns mark the results of a QSVR based on random encoding circuits (Sec. 3.1.2). The sixth category shows the results of an encoding circuit built by a genetic algorithm (Sec. 3.1.3).

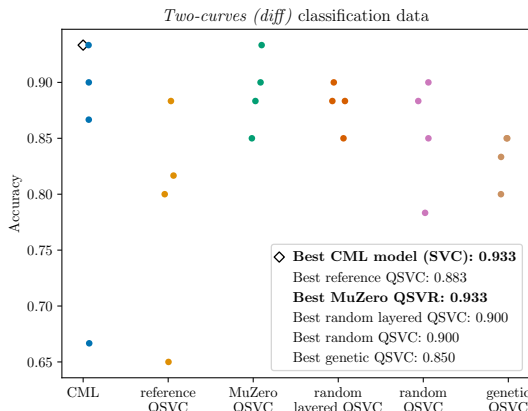


Fig. 4 Performance of the classification (Q)ML models on the *two-curves (diff)* test dataset. The columns follow the description in Fig. 3, with regression models replaced by classification models.

score on the test data. For this problem, the QSVC model, which is based on encoding circuits generated with the MuZero circuit search algorithm, and the classical SVM perform equally well with a test accuracy of 0.933. The reference circuits perform similarly to random circuits, with the best architecture for this problem being the optimized YZ-CX approach from Ref. [14]. The results of the genetic algorithm are below the two random search approaches.

Another important insight arises from the comparison with the random search routines and the genetic algorithm. The results from the QSVMs utilizing random encoding circuits are consistently positive across all cases and, on average, slightly outperform the reference encoding circuits. Encoding circuits build by genetic algorithms lag behind in Fig. 4). We found the layered structure to be beneficial over the flexible structure, not only when comparing the genetic algorithm to the MuZero circuit search, but also when comparing the two random search approaches with and without the layered structure.

We observed that in all cases there is a performance threshold that can be reached to a certain degree. We noted for both classical and QML models that a high training score does not consistently predict a high test score. Consequently, it is essential to design multiple circuits and evaluate them, as minor variations in cross-validated training scores can result in substantial differences in test scores. Conversely, poor cross-validation scores typically indicate significant generalization errors.

Due to the limited size of the data sets, SVR performed better than the other classical ML methods in two scenarios. This is advantageous for the comparison of QML and classical ML, since the QML models investigated in this study are essentially kernel methods. However, it is difficult to make predictions about the scaling behavior for

larger future problems. Especially in the area of big data, neural network approaches are starting to outperform their kernel-based counterparts.

These results underscore the main finding of this work: contrary to common practice in QML research, where reference circuit architectures are used and their parameters optimized, better results can be achieved with custom circuits. Notably, circuits created by a random search can yield already good outcomes, but the best possible performance was consistently achieved using the MuZero circuit search algorithm. This approach excels in learning from the problem structure, enabling the creation of tailored circuits that outperform other methods. Therefore, the MuZero circuit search algorithm is a reasonable choice for designing problem-specific quantum circuits, as it consistently produces the most effective solutions.

4 Discussion

In this study, we demonstrated the automatic generation of PQCs for QML using the MuZero circuit search algorithm. Our experiments illustrated the effectiveness of this RL framework in creating tailored circuits that considerably improve the performance of the QML model. The results consistently showed that these circuits outperformed the reference architectures from the literature. Interestingly, random search strategies also produce good results, often matching or even surpassing the performance of reference circuits from the literature. This is particularly notable given that reference circuits use optimized parameters, while the random search chooses these parameters randomly.

Although the presented QML models slightly outperform or match their classical counterparts, we do not claim an overall quantum advantage of the presented methodology, since all discussed datasets are relatively small compared to those that can be handled classically. The inherent complexity and variability of QML models make it difficult to establish consistent claims of performance advantages over classical ML models, especially when moving to larger datasets.

Looking forward, there are several opportunities to extend the workflow presented in this study. The MuZero circuit search algorithm can be adapted to generate circuits for different QML models, such as QNNs, and could serve as a general circuit optimization tool for other circuit

approaches outside of QML. Furthermore, incorporating operators that reflect the symmetries of the data set could introduce an informed inductive bias, leading to more practical circuit designs. Moreover, the MuZero circuit search is promising for transferring the learned RL model from one dataset to another, since the hidden state representation of the circuit has already been learned. Further research could evaluate the ability to generalize to new datasets without requiring intensive retraining of the RL algorithm.

In conclusion, our study highlights the significant potential of using reinforcement learning, in particular the MuZero circuit search algorithm, to generate problem-specific PQCs for QML. The results show that tailored circuits can significantly improve the performance of QML models and provide a solid foundation for future research and development in the field of QML.

Acknowledgments. We thank Jan Schnabel, Tobias Nagel and Philipp Wagner for insightful discussions. This work was supported by the Ministry of Economic Affairs, Labour, and Tourism Baden-Württemberg in the frame of the Competence Center Quantum Computing Baden-Württemberg (project SEQUOIA End-to-End).

References

- [1] Preskill, J. Quantum computing in the NISQ era and beyond. *Quantum* **2**, 79 (2018). URL <https://doi.org/10.22331/2Fq-2018-08-06-79>.
- [2] Cerezo, M., Verdon, G., Huang, H.-Y., Cincio, L. & Coles, P. Challenges and opportunities in quantum machine learning. *Nature Computational Science* **2** (2022).
- [3] Schuld, M. & Killoran, N. Quantum machine learning in feature hilbert spaces. *Physical Review Letters* **122** (2019). URL <https://doi.org/10.1103%2Fphysrevlett.122.040504>.
- [4] Lloyd, S., Schuld, M., Ijaz, A., Izaac, J. & Killoran, N. Quantum embeddings for machine learning (2020). URL <https://arxiv.org/abs/2001.03622>.
- [5] Benedetti, M., Lloyd, E., Sack, S. & Fiorenzini, M. Parameterized quantum circuits as

machine learning models. *Quantum Science and Technology* **4**, 043001 (2019). URL <https://doi.org/10.1088%2F2058-9565%2Fab4eb5>.

[6] Cerezo, M. *et al.* Variational quantum algorithms. *Nature Reviews Physics* **3**, 625–644 (2021). URL <http://arxiv.org/pdf/2012.09265v2.pdf>.

[7] Ragone, M. *et al.* A unified theory of barren plateaus for deep parametrized quantum circuits (2023). [2309.09342](https://arxiv.org/abs/2309.09342).

[8] Larocca, M. *et al.* A review of barren plateaus in variational quantum computing (2024). [2405.00781](https://arxiv.org/abs/2405.00781).

[9] Mitarai, K., Negoro, M., Kitagawa, M. & Fujii, K. Quantum circuit learning. *Phys. Rev. A* **98**, 032309 (2018). URL <https://link.aps.org/doi/10.1103/PhysRevA.98.032309>.

[10] Havlíček, V. *et al.* Supervised learning with quantum-enhanced feature spaces. *Nature* **567**, 209–212 (2019).

[11] Huang, H.-Y. *et al.* Power of data in quantum machine learning. *Nature Communications* **12** (2021). URL <https://doi.org/10.1038%2Fs41467-021-22539-9>.

[12] Hubregtsen, T. *et al.* Training quantum embedding kernels on near-term quantum computers (2021). URL <https://arxiv.org/abs/2105.02276>.

[13] Peters, E. *et al.* Machine learning of high-dimensional data on a noisy quantum processor (2021).

[14] Haug, T., Self, C. N. & Kim, M. S. Quantum machine learning of large datasets using randomized measurements. *Machine Learning: Science and Technology* **4**, 015005 (2023). URL <https://dx.doi.org/10.1088/2632-2153/acb0b4>.

[15] Havlíček, V. *et al.* Supervised learning with quantum-enhanced feature spaces. *Nature* **567**, 209–212 (2019). URL <https://doi.org/10.1038%2Fs41586-019-0980-2>.

[16] Farhi, E., Goldstone, J. & Gutmann, S. A quantum approximate optimization algorithm (2014). [1411.4028](https://arxiv.org/abs/1411.4028).

[17] Tilly, J. *et al.* The variational quantum eigensolver: A review of methods and best practices. *Physics Reports* **986**, 1–128 (2022). URL <https://www.sciencedirect.com/science/article/pii/S0370157322003118>. The Variational Quantum Eigensolver: a review of methods and best practices.

[18] Peruzzo, A. *et al.* A variational eigenvalue solver on a photonic quantum processor. *Nature Communications* **5**, 4213 (2014). URL <https://doi.org/10.1038/ncomms5213>.

[19] Skolik, A., McClean, J. R., Mohseni, M., van der Smagt, P. & Leib, M. Layerwise learning for quantum neural networks. *Quantum Mach. Intell.* **3**, 5 (2021).

[20] Wolpert, D. & Macready, W. No free lunch theorems for optimization. *IEEE Transactions on Evolutionary Computation* **1**, 67–82 (1997).

[21] Kübler, J. M., Buchholz, S. & Schölkopf, B. The inductive bias of quantum kernels (2021). [2106.03747](https://arxiv.org/abs/2106.03747).

[22] Bowles, J., Wright, V. J., Farkas, M., Killoran, N. & Schuld, M. Contextuality and inductive bias in quantum machine learning (2023). [2302.01365](https://arxiv.org/abs/2302.01365).

[23] Ragone, M. *et al.* Representation theory for geometric quantum machine learning (2023). [2210.07980](https://arxiv.org/abs/2210.07980).

[24] Larocca, M. *et al.* Group-invariant quantum machine learning. *PRX Quantum* **3**, 030341 (2022). URL <https://link.aps.org/doi/10.1103/PRXQuantum.3.030341>.

[25] Meyer, J. J. *et al.* Exploiting symmetry in variational quantum machine learning. *PRX Quantum* **4**, 010328 (2023). URL <https://link.aps.org/doi/10.1103/PRXQuantum.4.010328>.

[26] Schatzki, L., Larocca, M., Nguyen, Q. T., Sauvage, F. & Cerezo, M. Theoretical guarantees for permutation-equivariant quantum neural networks. *npj Quantum Inf.* **10**, 12 (2024).

[27] Gili, K., Alonso, G. & Schuld, M. An inductive bias from quantum mechanics: learning order effects with non-commuting measurements (2023). [2312.03862](https://arxiv.org/abs/2312.03862).

[28] Altares-López, S., Ribeiro, A. & García-Ripoll, J. J. Automatic design of quantum feature maps. *Quantum Science and Technology* **6**, 045015 (2021). URL <https://dx.doi.org/10.1088/2058-9565/ac1ab1>.

[29] Incudini, M. *et al.* Automatic and effective discovery of quantum kernels (2023). [2209.11144](https://arxiv.org/abs/2209.11144).

[30] Sünkel, L., Martyniuk, D., Mattern, D., Jung, J. & Paschke, A. Ga4qco: Genetic algorithm for quantum circuit optimization (2023). [2302.01303](https://arxiv.org/abs/2302.01303).

[31] Schrittwieser, J. *et al.* Mastering atari, go, chess and shogi by planning with a learned model. *Nature* **588**, 604–609 (2020). URL <http://dx.doi.org/10.1038/s41586-020-03051-4>.

[32] Świechowski, M., Godlewski, K., Sawicki, B. & Mańdziuk, J. Monte carlo tree search: a review of recent modifications and applications. *Artificial Intelligence Review* **56**, 2497–2562 (2023). URL <https://doi.org/10.1007/s10462-022-10228-y>.

[33] Pozzi, M. G., Herbert, S. J., Sengupta, A. & Mullins, R. D. Using reinforcement learning to perform qubit routing in quantum compilers. *ACM Transactions on Quantum Computing* **3** (2022). URL <https://doi.org/10.1145/3520434>.

[34] Ruiz, F. J. R. *et al.* Quantum circuit optimization with alphatensor (2024). [2402.14396](https://arxiv.org/abs/2402.14396).

[35] Ostaszewski, M., Trenkwalder, L. M., Masarczyk, W., Scerri, E. & Dunjko, V. Ranzato, M., Beygelzimer, A., Dauphin, Y., Liang, P. & Vaughan, J. W. (eds) *Reinforcement learning for optimization of variational quantum circuit architectures*. (eds Ranzato, M., Beygelzimer, A., Dauphin, Y., Liang, P. & Vaughan, J. W.) *Advances in Neural Information Processing Systems*, Vol. 34, 18182–18194 (Curran Associates, Inc., 2021). URL https://proceedings.neurips.cc/paper_files/paper/2021/file/9724412729185d53a2e3e7f889d9f057-Paper.pdf.

[36] Altmann, P. *et al.* Challenges for reinforcement learning in quantum circuit design (2024). [2312.11337](https://arxiv.org/abs/2312.11337).

[37] Gil-Fuster, E., Eisert, J. & Dunjko, V. On the expressivity of embedding quantum kernels. *Machine Learning: Science and Technology* **5**, 025003 (2024). URL <https://dx.doi.org/10.1088/2632-2153/ad2f51>.

[38] Schuld, M., Sweke, R. & Meyer, J. J. Effect of data encoding on the expressive power of variational quantum-machine-learning models. *Physical Review A* **103** (2021). URL <https://doi.org/10.1103/PhysRevA.103.032430>.

[39] Schuld, M. Supervised quantum machine learning models are kernel methods (2021). URL <https://arxiv.org/abs/2101.11020>.

[40] Nguyen, Q. T. *et al.* Theory for equivariant quantum neural networks. *PRX Quantum* **5**, 020328 (2024). URL <https://link.aps.org/doi/10.1103/PRXQuantum.5.020328>.

[41] Sutton, R. S. & Barto, A. G. *Reinforcement learning: An introduction* (MIT press, 2018).

[42] Schulman, J., Wolski, F., Dhariwal, P., Radford, A. & Klimov, O. Proximal policy optimization algorithms (2017). [1707.06347](https://arxiv.org/abs/1707.06347).

[43] García, C. E., Prett, D. M. & Morari, M. Model predictive control: Theory and practice—a survey. *Automatica* **25**, 335–348 (1989). URL <https://www.sciencedirect.com/science/article/pii/0005109889900022>.

[44] Kreplin, D. A., Willmann, M., Schnabel, J., Rapp, F. & Roth, M. sklearn — a python

library for quantum machine learning (2023). [2311.08990](#).

- [45] Akiba, T., Koyama, M. *et al.* Optuna: A next-generation hyperparameter optimization framework. *Proceedings of the 25th ACM SIGKDD International Conference on Knowledge Discovery and Data Mining* (2019).
- [46] Bowles, J., Ahmed, S. & Schuld, M. Better than classical? the subtle art of benchmarking quantum machine learning models (2024). [2403.07059](#).
- [47] Glick, J. R. *et al.* Covariant quantum kernels for data with group structure. *Nature Phys.* **20**, 479–483 (2024).
- [48] Chen, T. & Guestrin, C. Xgboost: A scalable tree boosting system. *Proceedings of the 22nd ACM SIGKDD International Conference on Knowledge Discovery and Data Mining* (2016). URL <http://dx.doi.org/10.1145/2939672.2939785>.
- [49] Abadi, M., Zheng, X. *et al.* TensorFlow: Large-scale machine learning on heterogeneous systems (2015). URL <https://www.tensorflow.org/>. Software available from tensorflow.org.
- [50] Pedregosa, F., Duchesnay, E. *et al.* Scikit-learn: Machine learning in Python. *Journal of Machine Learning Research* **12**, 2825–2830 (2011).
- [51] Xiao, H., Rasul, K. & Vollgraf, R. Fashion-mnist: a novel image dataset for benchmarking machine learning algorithms (2017). [1708.07747](#).